

Pressure measurements and an analytical model for laser-generated shock waves in solids at low irradiance

This article has been downloaded from IOPscience. Please scroll down to see the full text article.

2002 J. Phys.: Condens. Matter 14 10793

(<http://iopscience.iop.org/0953-8984/14/44/379>)

View [the table of contents for this issue](#), or go to the [journal homepage](#) for more

Download details:

IP Address: 171.66.16.97

The article was downloaded on 18/05/2010 at 17:11

Please note that [terms and conditions apply](#).

Pressure measurements and an analytical model for laser-generated shock waves in solids at low irradiance

J P Romain¹, F Bonneau², G Dayma¹, M Boustie¹, T de Rességuier¹ and P Combis²

¹ Laboratoire de Combustion et de Détonique, ENSMA, BP 40109, 86961 Futuroscope-Chasseneuil Cedex, France

² Département de Physique Théorique et Appliquée CEA/DAM Ile de France, BP 12, 91680 Bruyères le Châtel, France

E-mail: romain@ensma.fr

Received 13 June 2002

Published 25 October 2002

Online at stacks.iop.org/JPhysCM/14/10793

Abstract

Low amplitude shock waves (from 1 to 300 bar) have been generated in gold layers deposited on a quartz substrate, by laser pulses at an incident fluence from 0.4 to 4.0 J cm⁻². The quartz was used as a pressure gauge for recording the induced shock profile. At a fluence < 1.4 J cm⁻², the shock pressure does not exceed 10 bar and the shock front is followed by a tension peak typical of an absorption in solid state. An analytical model of the compression–tension process has been developed, accounting for shock pressure and shock profile evolution as a function of irradiation conditions and material properties. From this model a mechanical interpretation is given to previous observations of spalling of the irradiated target surface.

(Some figures in this article are in colour only in the electronic version)

1. Introduction

Laser shocks are usually generated in solids by the plasma produced by absorption of incident radiation at the target surface. At very high laser intensity, pressures in the TPa range may be achieved [1–3]. Conversely, at low irradiance, if the absorbed energy does not reach the vapourization threshold, the target surface is kept in solid state and the pressure increase is very small. In such conditions a typical shock effect has been observed in the form of thin spalls (μm thickness) of the irradiated surface [4]. In the present study we propose an interpretation of this effect based on records of shock profiles and completed by an analytical model describing the compression–tension process at the origin of spalling.

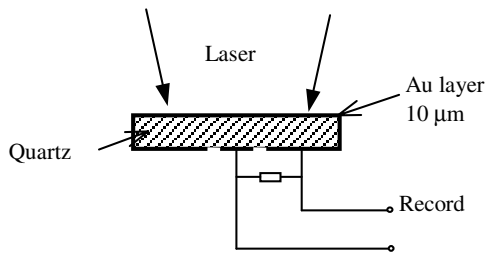


Figure 1. Experimental configuration.

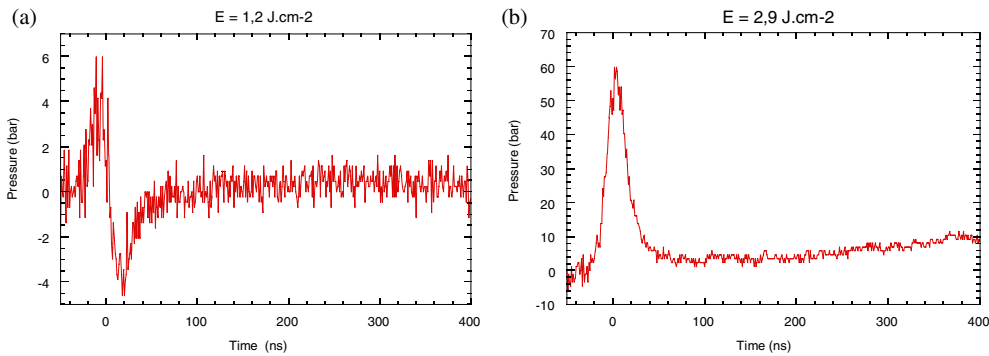


Figure 2. Records of shock profiles induced by absorption in solid state (a), and vapour/plasma state (b).

2. Experimental details

The targets consisted of thin gold layers ($10\ \mu\text{m}$) deposited on a quartz substrate. The temporal shock profiles have been recorded by means of the piezoelectric response of quartz used as a pressure gauge (figure 1). The irradiation conditions were: $1.06\ \mu\text{m}$ laser wavelength, pulses of $25\ \text{ns}$ duration (FWHM), and incident fluence from 0.4 to $4.0\ \text{J cm}^{-2}$.

The pressure records reveal two types of profile depending on the range of laser intensity. At a fluence $< 1.4\ \text{J cm}^{-2}$, the induced peak pressure does not exceed $10\ \text{bars}$ and the compression front is followed by a tension peak characteristic of an absorption of energy in solid state (figure 2(a)). At a fluence $> 1.4\ \text{J cm}^{-2}$ the tension peak disappears (figure 2(b)) and the pressure increase is much stronger (up to $300\ \text{bars}$ at $4.0\ \text{J cm}^{-2}$). This profile is typical of an absorption in vapour/plasma state.

The experimental points of peak shock pressure as a function of incident fluence are displayed in figure 3, evidencing the vapourization threshold at about $1.4\ \text{J cm}^{-2}$. In the regime of absorption in solid state the induced pressure and resulting signal amplitude are very low. The signal/noise ratio of the quartz response is near unity, inducing a poor accuracy on the measurements. However, the experimental results indicate a linear dependence of shock pressure on laser fluence, at an approximate rate of $3.5\ \text{bar J}^{-1}\ \text{cm}^{-2}$.

3. Analytical model

A model based on the mechanics of shock and release waves propagating through the target is proposed for predicting the shock profile evolution as a function of irradiation conditions. The energy is supposed to be absorbed at the solid surface in a thickness e related to heat conduction in the material. For the purpose of this analysis the laser pulse is approximated by a symmetric

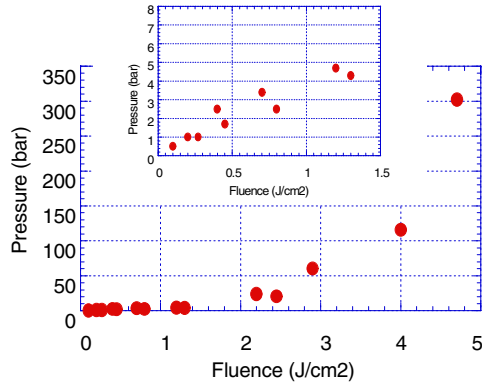


Figure 3. Peak shock pressure transmitted in the quartz gauge versus incident laser fluence.

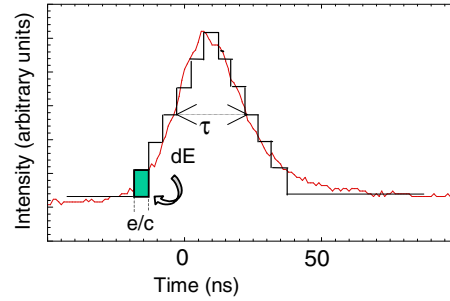


Figure 4. Stepped profile model of the laser pulse.

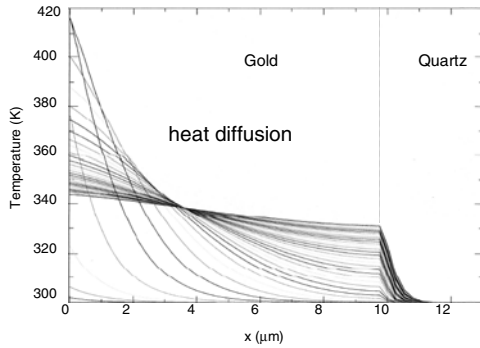


Figure 5. Computed evolution of temperature in the target irradiated at 1.2 J cm^{-2} , for $0 < t < 350 \text{ ns}$. The irradiated surface is at $x = 0$. The effective absorption depth is defined as the temperature gradient length: $e \approx 3 \mu\text{m}$.

stepped profile (figure 4). The width of each step is e/c , where c represents the sound velocity in the material. The energy per unit area transported in each elementary step is designed by dE , from which $(1 - R) dE$ is absorbed in the material. R is the material reflectivity.

The associated pressure increase dP is then derived from the Mie–Grüneisen equation of state and from the relation between the laser pulse energy E , the laser pulse length τ , and the transit time e/c . In our experimental conditions $e/c \ll \tau$, so

$$dP = \frac{\Gamma e}{\tau^2 c^2} (1 - R) E \quad (1)$$

where Γ is the Grüneisen coefficient of the material. For gold, $\Gamma = 3.1$, $c = 3250 \text{ m s}^{-1}$, R is assumed to be about 0.89 and $e = 3 \mu\text{m}$ is an average and approximate value estimated from numerical simulations of laser–matter interaction [5] (figure 5). Then dP (bar) = $15.5 E$ (J cm^{-2}).

The successive states in the absorption zone are represented in space–time and pressure–material velocity diagrams as shown in figures 6 and 7. For simplification the construction is made with a three-step increasing and decreasing loading profile.

This construction evidences alternated areas of compression (1, a, c, e, g, h) and tension (b, d, f) in the absorption zone as a consequence of successive reverberations at both edges of this zone. The resulting stress history at interface between the absorption zone and the rest of the target (cold target) is then composed of a square compression pulse (state 1) of duration equal to that of the laser pulse, followed by a symmetrical tension pulse (state b). This shock

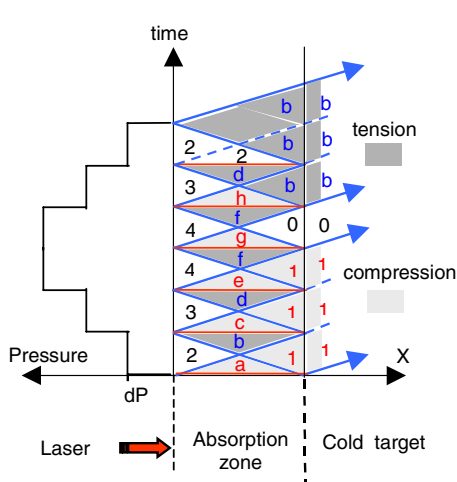


Figure 6. Space–time diagram of shock and release waves in the absorption zone. The numbers refer to states determined in the pressure–material velocity diagram of figure 7.

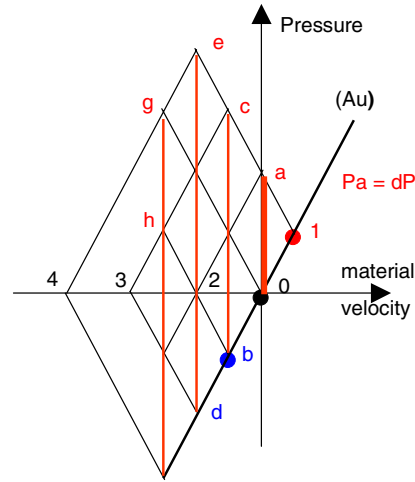


Figure 7. Pressure–material velocity diagram of the successive states in the absorption zone.

profile is transmitted into the cold part of the target and finally into the quartz gauge. As the transmission ratio from gold to quartz is $2Z_Q/(Z_{Au} + Z_Q)$, where Z_Q and Z_{Au} are respectively the shock impedances of quartz and gold, and because $P_1 = dP/2$ (figure 7), the amplitude P_Q of the shock (and symmetrically of the tension) transmitted into the gauge is

$$P_Q = \frac{Z_Q}{Z_{Au} + Z_Q} dP. \quad (2)$$

From equations (1) and (2), with $Z_Q = 1.52 \times 10^7 \text{ Pa s m}^{-1}$ and $Z_{Au} = 6.24 \times 10^7 \text{ Pa s m}^{-1}$, we get

$$P_Q \text{ (bar)} = 3.0E \text{ (J cm}^{-2}\text{)}. \quad (3)$$

The linear energy dependence of pressure predicted from equation (3) correctly fits the experimental results (figure 3). In figure 8 the experimental record of figure 2(a) is compared with the theoretical profile inferred from the constructions of figures 6, 7 and from a numerical application of equation (3) at 1.2 J cm^{-2} incident fluence. It shows that the main features of the record (profile, amplitude and duration) are well reproduced by the model. The tensile stress amplitude is directly related to that of the leading shock and is only a few bars in this absorption regime. However, it may be strong enough for producing a fracture and a spalling of the material at the interface between absorption zone and cold target, which is indeed a region of increased fragility due to high temperature gradient and high shear stress.

4. Conclusions

Experimental records of shock profiles generated by laser pulses at an irradiance lower than the vapourization threshold confirm the existence of tensile stress, as expected from previous observations of related spalling effects. An analytical model describing the compression–tension process involved in these experiments has been developed, and the pertinent parameters have been identified. The linear relationship between applied shock pressure and incident

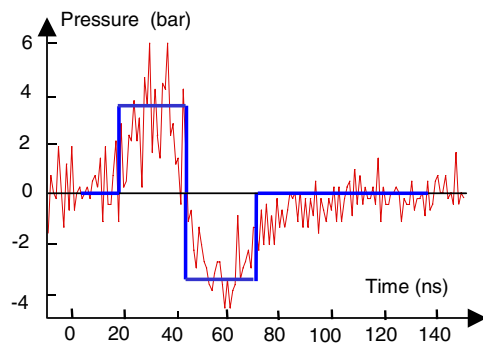


Figure 8. Experimental (thin curve) and calculated (thick curve) shock profile transmitted from gold to quartz at 1.2 J cm^{-2} incident fluence.

energy derived from the model correctly fits the experimental results and appears to be very useful for analysing the influence of laser irradiation conditions and material parameters on induced peak pressures. Additional measurements, especially on material reflectivity, should be made in order to increase the accuracy of the model predictions. Further numerical simulations coupling laser–matter interaction, hydrodynamics, elastoplasticity and heat conduction will provide a complete and detailed understanding of the whole process. Finally it should be mentioned that the spalling mechanism described in this model could be involved in some conditions of the laser technique application to surface cleaning of materials.

References

- [1] Cottet F, Romain J P, Fabbro R and Faral B 1984 *Phys. Rev. Lett.* **52** 1884
- [2] Cauble R, Phillion D W, Hoover T J, Holmes N C, Kilkenny J D and Lee R W 1993 *Phys. Rev. Lett.* **70** 2102
- [3] Koenig M, Faral B, Boudenne J M, Batani D, Bossi S, Benuzzi A, Remond C, Perrine J, Temporal M and Atzeni S 1995 *Phys. Rev. Lett.* **74** 2260
- [4] Dubern C 1999 *Thesis* Universite Bordeaux 1
- [5] Combis P, Bonneau F and Lamagnère L 2000 *Proc. SPIE* **3902** 317–23